Neoplasma 2024; 71(6): 559–570

doi:10.4149/neo_2024_240803N328

circ_0075829 regulates ferroptosis and immune escape in colon cancer cells through the miR-330-5p/TCF4 axis

Huajun FAN[1], Yu DING[2], Zhe XIAO[3], Shengbo LI[3], Yongbin ZHENG[3,*]

[1]Department of Plastic Surgery, Renmin Hospital of Wuhan University, Wuchang, Wuhan, Hubei, China; [2]Pain Department, Renmin Hospital of Wuhan University, Wuchang, Wuhan, Hubei, China; [3]Department of Gastrointestinal Surgery, Renmin Hospital of Wuhan University, Wuchang, Wuhan, Hubei, China

**Correspondence: zhengyongbinzyb@21cn.com*

Received August 3, 2024 / Accepted December 6, 2024

Many lines of evidence suggest that circular RNAs (circRNAs) are closely associated with the occurrence and progression of colon cancer. The objective of this study was to investigate the regulatory effects and mechanisms of circ_0075829 on ferroptosis and immune escape in colon cancer. We utilized colon cancer cell lines and a xenograft mouse model to analyze the function of circ_0075829 *in vitro* and *in vivo*. The gene expression level was assessed by qRT-PCR and western blotting. Cell proliferation was evaluated using the CCK-8 assay. The targeting relationships between circ_0075829, miR-330-5p, and TCF4 were analyzed through a dual-luciferase reporter experiment and RNA pull-down experiment. Cytokine levels were measured using the ELISA assay. Fe^{2+}, MDA, and SOD levels were tested using appropriate kits, and the ROS level was detected by immunofluorescence. Knockdown of circ_0075829 resulted in increased levels of Fe^{2+}, ROS, and MDA and decreased levels of GPX4 and xCT proteins in cells. Furthermore, silencing of circ_0075829 increased the cell proliferation rates of CD8+T cells co-cultured with colon cells. Moreover, it also enhanced IFN-γ, IL-2, and TNF-α concentration in the supernatants of the co-culturing system and reduced PD-L1 protein expression levels. Subsequently, silencing of circ_0075829 induced ferroptosis and inhibited immune escape *in vivo*. Meaningfully, we certified that circ_0075829 functions as a sponge for miR-330-5p, leading to the upregulation of TCF4 expression. TCF4 was identified as a downstream target of miR-330-5p. Additionally, co-transfection with anti-miR-330-5p or TCF4 overexpression plasmid reversed the effects observed following the knockout of circ_0075829. Collectively, our research indicates that the circ_0075829 plays a significant role in regulating ferroptosis and immune escape in colon cancer by sponging miR-330-5p to modulate TCF4 expression.

Key words: colon cancer; circ_0075829; miR-330-5p; TCF4; ferroptosis; immune escape

Colon cancer, a malignant tumor of the digestive system, is prevalent among the Chinese population, with rectal cancer being the most common subtype [1]. The pathogenesis of the disease remains unclear, but it is believed to be influenced by environmental factors, diet, and genetic predispositions [2]. Despite rapid advancements in clinical therapies for colon cancer over recent years, prognostic outcomes have not been satisfactory [3]. Therefore, identifying new therapeutic targets remains critically important for patients with colon cancer. Recent studies have indicated that ferroptosis may play a regulatory role in the progression and treatment of various cancers [4]. Increasing studies have demonstrated that certain genes associated with ferroptosis can serve as the prognostic indicators in colon cancer [5, 6]. Additionally, immune escape is an extremely crucial process in the development of colon cancer [7]. Nevertheless, many unresolved issues persist regarding the regulatory mechanisms underlying ferroptosis and immune escape and their implications for colon cancer management.

Circular RNA (circRNA) is a multifunctional molecule that plays a significant role in cancer development and metastasis [8]. An increasing body of research has identified circRNAs as an important class of biomarkers in colon cancer. For example, circ_0055625 has been found to promote tumor growth in colon cancer, thus serving as a potential biomarker for this disease [9]. In addition, hsa_circ_0004585 exhibits high expression levels in colorectal cancer (CRC) patients, possesses carcinogenic properties, and is associated with cancer metastasis [10]. A classifier based on circRNA can serve as an effective prognostic tool for predicting postop-

erative tumor recurrence in patients with stage II/III colon cancer [11]. circ_0075829 is formed by reverse splicing of LINC00340. LINC00340, also known as CASC15, is a long non-coding RNA gene located on human chromosome 6 [12]. CASC15 has been closely linked to the occurrence and progression of various cancers, including colon cancer [13]. Although there are limited studies regarding the role of circ_0075829 in oncology, one study indicated that circ_0075829 shows increased expression levels in pancreatic cancer tissue based on circRNA microarray data [14]. Furthermore, recent research reported that the expression of circ_0075829 was significantly elevated in pancreatic cancer tissues and functions as an oncogene [15]. However, overexpression of circ_0075829 in neuroblastoma appears to inhibit cell proliferation and migration, and its high expression correlates with favorable clinical phenotype [16]. Nonetheless, the regulatory function of circ_0075829 in colon cancer and its underlying mechanism remains unexplored.

MicroRNAs (miRNAs) are intricately associated with the occurrence, development, diagnosis, treatment, prognosis, and other aspects of various diseases, including cancer [17]. miRNA is particularly linked to the occurrence, progression, and treatment of colon cancer [18]. Numerous studies have indicated that circRNAs, functioning as molecular sponges for miRNAs, possess multiple binding sites for miRNAs. Consequently, circRNAs can moderate the inhibitory effects of miRNAs on their target genes and enhance their expression [19]. For example, it has been demonstrated that circCTNNA1 can counteract the inhibitory effect of miR-149-5p on FOXM1, and the targeting relationship between circCTNNA1, miR-149-5p, and FOXM1 promotes proliferation and invasion in CRC cells [20]. Furthermore, research has shown that the expression of miR-330-5p decreases in colon cancer where it functions as a tumor suppressor gene [21]. The miR-330 gene is located on human chromosome 19 [22] and plays an important role in the pathogenesis of various cancers. miR-330-5p belongs to the miR-330 family. Several investigations have revealed that miR-330-5p can be regulated by circRNAs to affect the phenotype of colon cancer. For example, Zhao et al. [23] indicated that miR-330-5p was the target of circRNA_000166 and regulated cell proliferation, migration, and invasion in colon cancer. Moreover, the inhibitory effects of miR-330-5p on CRC cell proliferation and metastasis were mitigated by the upregulation of circ-FARSA [24]. Based on the prediction from CircInteractome, we hypothesize that circ_0075829 acts as a sponge for miR-330-5p. Nevertheless, the action of circ_0075829 and miR-330-5p in colon cancer needs to be further studied.

The objective of our research was to investigate the biological role of circ_0075829 in colon cancer ferroptosis and immune escape, as well as to further examine the correlations among circ_0075829, miR-330-5p, and TCF4. The findings may offer a potentially significant therapeutic approach for clinical treatment and prognosis in colon cancer.

Materials and methods

Cell culture and transfection. HCT116 and SW480, human colon cancer cell lines, were obtained from the Cell Bank of the Chinese Academy of Sciences (#TCHu99 and TCHu172, Shanghai, China). The cells were cultured in DMEM (#11995065, Gibco, MA, USA) supplemented with 10% fetal bovine serum (#10099, Gibco) with 5% CO_2 at 37 °C.

The circ_0075829 silencing (sh-circ_0075829) and negative control (sh-NC), miR-330-5p overexpression (miR-330-5p mimic) and its corresponding negative control (miR-NC), antisense RNA against miR-330-5p (anti-miR-330-5p) and its control (anti-NC), lentiviral vector of TCF4 were provided by RiboBio (Guangzhou, China). Transfection was performed using a Lipofectamine 2000 transfection kit (#11668-019, Invitrogen, Carlsbad, USA) in accordance with the manufacturer's specifications. The oligos sequences are shown in Supplementary Table S1.

Fe^{2+}, MDA, and SOD levels. The Iron Assay, MDA, and SOD test kits (#ab83366, Abcam, UK; #S0131 and #S0101, Beyotime, Shanghai, China) were utilized to measure the levels of Fe^{2+}, MDA, and SOD in sample cells, respectively. The specific experimental procedures were conducted strictly according to the instructions of the kit. This assay was performed in triplicate.

Lipid ROS detection. The level of lipid reactive oxygen species (ROS) was assessed using the C11-BODIPY 581/591 kit (#D3861, Thermo Fisher Scientific, Waltham, MA, USA). In brief, HCT116 and SW480 cells were seeded in 6-well plates at a density of 5×10^4 cells/well) for 24 h and subsequently incubated with 2 μM C11-BODIPY 581/591 for 30 min. The cells were then examined using a laser scanning confocal microscope and analyzed with ImageJ. The oxidized BODIPY (O-BODIPY) and reduced BODIPY (R-BODIPY) were detected at excitation/emission wavelengths of 488/510 (traditional FITC filter set) and 581/591 nm (Texas Red filter set), respectively. Three replicates were performed for each process.

Western blotting (WB). SDS-PAGE gel (#CW0022, CWBIO, Beijing, China) separated equivalent protein extracted from HCT116 and SW480 cells. Subsequently, these samples were transferred onto PVDF membranes (#JKA40001, OKA, Beijing, China) and treated with defatted milk. The membranes were then incubated with primary antibodies at 4 °C overnight and treated with horseradish peroxidase-conjugated goat anti-rabbit IgG second antibody (#ab205718, 1:1500, Abcam, Cambridge, UK) at room temperature. After 1 h, ECL and ImageJ were applied to visualize and analyze the protein bands. The primary antibodies employed in this study are shown below: anti-GPX4 (#ab125066, 1:1000, Abcam), anti-xCT (#ab37185, 1:500, Abcam), anti-PD-L1 (#ab213480, 1:1000, Abcam), anti-TCF4 (#ab185736, 1:1000, Abcam), anti-GAPDH (#ab181602, 1:2000, Abcam). This assay was carried out at least three times.

Immune escape assay. The peripheral blood mononuclear cells (PBMCs) were isolated from the peripheral blood of healthy volunteers using Ficoll density gradient centrifugation. Easy-Sep™ Direct Human CD8+ T cell Isolation Kit (#550583, STEMCELL Technologies, Canada) was employed to acquire CD8+ T cells. These cells were cultured in RPMI-1640 medium and activated by anti-CD3/anti-CD28 antibodies (#10970, STEMCELL) and IL-2 (#78036, STEMCELL) for 48 h. HCT116 and SW480 cells that had undergone different transfection treatments were co-cultured with the activated CD8+ T cells at a ratio of 1:10 for 48 h. Based on the growth characteristics of both suspended CD8+ T cells and adherent tumor cells, the suspended CD8+ T cells were directly harvested by centrifugation for subsequent experiments. The tumor cells adhering to the wall were digested with trypsin before being collected through centrifugation. The viability of CD8+ T cells was assessed using the Cell Count Kit-8 assay (CCK-8, #CA1210, Solarbio, Beijing, China). Subsequently, levels of IFN-γ, IL-2, and TNF-α in the supernatants from the co-culturing system were quantified using commercial ELISA kits (#ab174443, #ab46054 and #ab208348, Abcam). This experiment was repeated in triplicate.

Construction of xenograft mouse model. All procedures involving animal experiments were approved by the Ethics Committee of Renmin Hospital of Wuhan University (Hubei, China, Approval No. 202205). The huPBMC-NOG-dKO female mice were obtained from Vital River Laboratory Animal Technology (Beijing, China). The xenograft tumor model was established following previously published literature [25, 26]. These mice were housed in filter-top cages with no more than six in each cage under a constant 12 h light/dark cycle at 24±2°C and 40–60% relative humidity. The mice had free access to feed and water at any time. All mice were acclimated for two weeks before the experiment. They were then randomized into two groups (N=6 for each group). The dorsal flanks of the mice were disinfected three times with 75% alcohol. One group received subcutaneous injections of 6×10^6 (100 μl of PBS) colon cancer cells transfected with sh-circ_0075829. The other group was injected with an equal volume containing sh-NC cells by the same method. The vital signs of the mice were monitored once a week after injection. After 5 weeks, xenograft mouse models were sacrificed via cervical dislocation [27] and complete tumor samples were collected. The whole experiment was carried out in specific pathogen-free conditions.

Hematoxylin and eosin (H&E) staining. The excised tumor tissues were treated with formaldehyde and subsequently embedded in paraffin (#A56132, OKA). The sections were stained with H&E and observed using light microscopy to verify the tumor tissues. The experiment was conducted with six tumor tissue samples.

Immunohistochemistry (IHC). The paraffin-embedded tissues were sectioned into 4 mm slices, dewaxed, and rehydrated. Subsequently, the sections were incubated with the primary antibody GPX4 (#ab125066, Abcam), xCT (#ab37185, Abcam), PD-L1 (#ab228415, Abcam), IFN-γ (#ab25101, Abcam), and CD8 (#ab93278, Abcam) overnight at 4°C. Following incubation with a secondary antibody, the sections were stained with DAB (#SFQ004, 4A Biotech, Beijing, China) and counterstained with hematoxylin (#D10519, OKA). Staining intensity was scored as follows: 0 (negative), 1 (weak), 2 (moderate), and 3 (strong). The staining area was scored as follows: 0 (0), 1 (1–25%), 2 (26–50%), 3 (51–75%), and 4 (76–100%). The above procedure was performed independently by two experienced pathologists. An Olympus microscope was used to observe the expression image of GPX4, xCT, PD-L1, IFN-γ, and CD8 in the tissue sections. This assay was conducted on six tumor tissue samples.

Dual-luciferase reporter experiment. The wild-type fragments of circ_0075829 (circ_0075829-wt: 5'-CACACGCAUGGAAAACCCAGAGG-3') and TCF4 (TCF4-wt: 5'-GGCUGAGACACAGCCCAGAGA-3') and corresponding mutant sequence (circ_0075829-mut: 5'-CACACGCAUGGAAAAGGGUCUCG-3' and TCF4-mut: 5'-GGCUGUCUGUGUCGGGUCUCA-3') were inserted into the luciferase reporter vector pmirGLO (cat. no. E1330, USA). Then, these luciferase vectors were co-transfected with miR-330-5p mimic and NC mimic into HCT116 and SW480 cells using Lipofectamine 2000. After 48 h, the luciferase activity was measured utilizing a Dual-Luciferase Reporter Assay kit (#RG027, Beyotime). The experiment was repeated three times.

RNA pull-down experiment. HCT116 and SW480 cells were lysed using lysis buffer and incubated with a biotin-labeled circ_0075829 probe (bio-circ_0075829, Genepharm, Shanghai, China) and negative control probe (Bio-NC, Genepharm) for 48h, respectively. Then the cells were enriched using streptavidin-anchored magnetic beads (#11206D, Invitrogen). After thoroughly washing the beads, the pull-down complex was collected to assess the enrichment of miR-330-5p via qRT-PCR. All procedures were repeated 3 times.

qRT-PCR. TRIzol reagent (#15596-026, Invitrogen) was utilized for the total extraction of RNA from HCT116 and SW480 cells. The commercial kit (#4366596, Thermo) was employed to inverse-transcribe miRNA into cDNA. The entire qRT-PCR process was conducted using the ABI 7500 Fast Real-Time PCR System. U6 and β-actin served as the internal references, and results were calculated using the $2^{-\Delta\Delta Ct}$ method. The primers are listed in Supplementary Table S2. The experiment was repeated in triplicate.

Statistical analysis. In our study, statistical analysis was conducted using SPSS (version 21.0). Data are presented as mean ± standard deviation (SD). The differences between the two groups were compared using Student's t-test, while comparisons among multiple groups were performed with a one-way ANOVA. A p-value <0.05 manifested that the difference was statistically significant.

Results

Knockdown of circ_0075829 induced ferroptosis *in vitro*. To investigate the impact of circ_0075829 on ferroptosis in colon cancer cells (HCT116 and SW480), we silenced circ_0075829 in both HCT116 and SW480 cells (Figure 1A). Compared with cells transfected with sh-NC, sh-circ_0075829#3 was selected because it had the highest interference efficiency and could not generate remarkable effects on the expression of CASC15 (Supplementary Figure S1). It is well known that levels of Fe^{2+}, ROS, MDA, and SOD in cells will change during ferroptosis [28]. Notably, compared with the negative control group (sh-NC), the Fe^{2+} level was significantly increased in the sh-circ_0075829 group

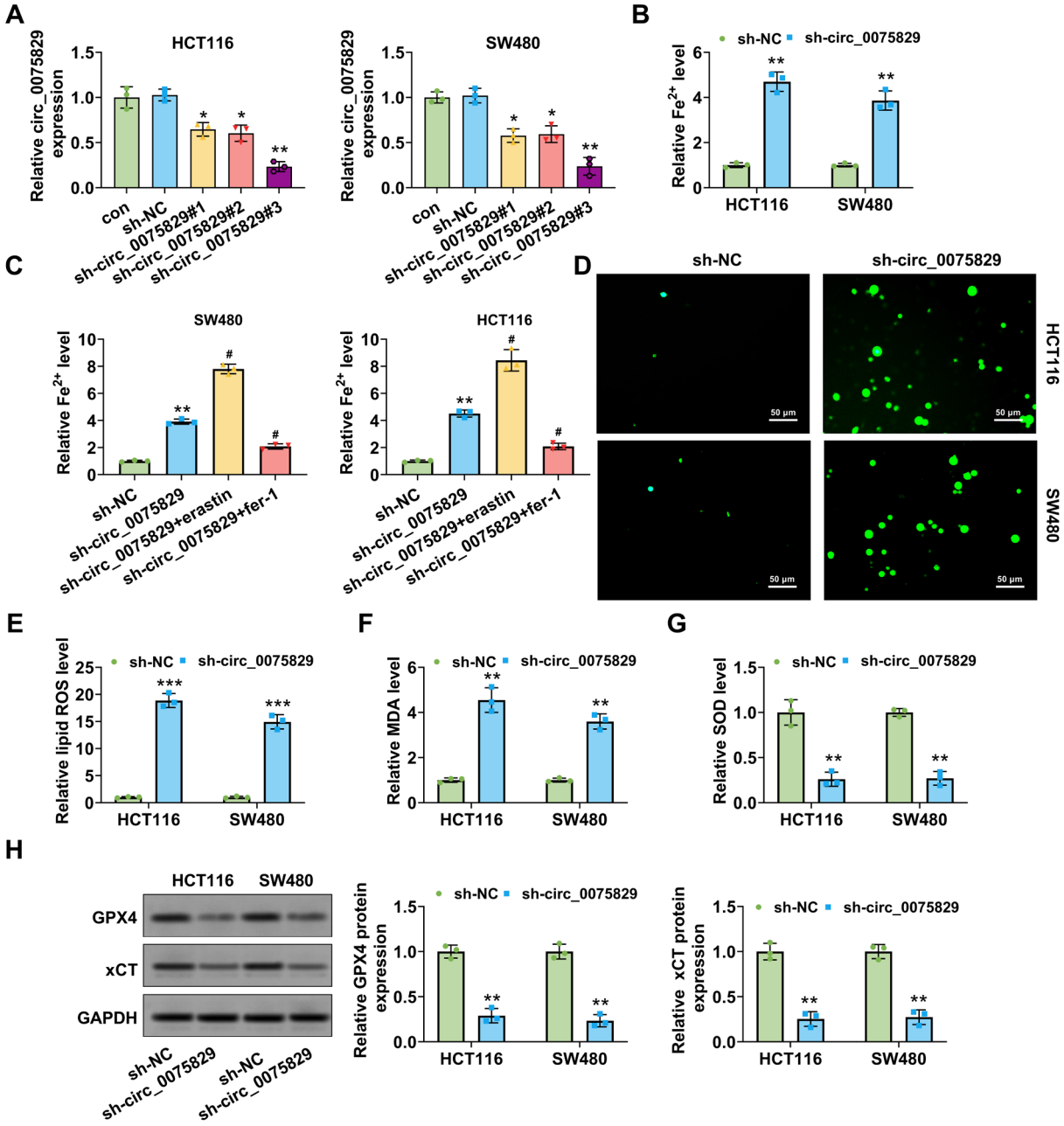

Figure 1. The effects of circ_0075829 on ferroptosis in colon cancer cells. sh-circ_0075829 was transfected into HCT116 and SW480 cells. A) qRT-PCR was used to detect the relative expression level of circ_0075829. B) Relative level of Fe^{2+} in cells. C) Relative level of Fe^{2+} in sh-circ_0075829 cells treated with erastin and ferrostatin-1 (fer-1). D–E) Relative level of lipid ROS in cells. (F) Relative level of MDA in cells. G) Relative level of SOD in cells. H) Relative expression level of GPX4 and xCT protein in cells was estimated by WB blotting. N=3. Compared with sh-NC *p<0.05, **p<0.01. Compared with sh-circ_0075829 ***p<0.001. #p<0.05, ##p<0.01, ###p<0.001

(Figure 1B). To further elucidate the role of circ_0075829 in cell ferroptosis, we treated the cells with erastin (ferroptosis inducer) and Fer-1 (Ferrostatin-1, ferroptosis inhibitor), respectively. In comparison to the sh-circ_0075829 group, the Fe^{2+} level was obviously increased in sh-circ_0075829 + erastin but decreased in the sh-circ_0075829 + fer-1 group (Figure 1C). Additionally, we observed that ROS levels were prominently higher in the sh-circ_0075829 group than in the sh-NC group ($p<0.01$, Figures 1D, 1E). The MDA level was also elevated in sh-circ_0075829 cells (Figure 1F). However, the SOD level was reduced in sh-circ_0075829 cells compared with sh-NC cells (Figure 1G). GPX4 and xCT are critical proteins that prevent ferroptosis, and their protein levels and activity directly affect the occurrence of ferroptosis [29]. The relative expression levels of GPX4 and xCT protein were remarkably decreased in the sh-circ_0075829 group (Figure 1H). In summary, these findings demonstrated that the knockdown of circ_0075829 induced ferroptosis in colon cancer cells.

Knockdown of circ_0075829 inhibited immune escape in colon cancer cells. To investigate the potential impact of circ_0075829 on immune escape, we co-cultured sh-circ_0075829 colon cancer cells and CD8+ T cells for 24 h. Compared to the sh-NC group, there was an increase in CD8+T cell proliferation in the sh-circ_0075829 group (Figure 2A). The concentrations of IFN-γ, IL-2, and TNF-α were elevated in the supernatants from the co-culturing system involving CD8+ T cells and sh-circ_0075829 colon cancer cells (Figures 2B–2D). Furthermore, compared with sh-NC cells, PD-L1 protein expression was significantly reduced in sh-circ_0075829 cells (Figure 2E). These findings suggested that the knockdown of circ_0075829 inhibited immune escape in colon cancer cells.

Knockdown of circ_0075829 induced ferroptosis and inhibited immune escape *in vivo*. To investigate the influence of circ_0075829 on ferroptosis and immune escape *in vivo*, we established a xenograft tumor model of colon cancer. Firstly, compared to the sh-NC group, both the subcutaneous tumor volume and weight were significantly reduced in the sh-circ_0075829 group ($p<0.01$, Figures 3A, 3B). Knockdown of circ_0075829 notably decreased the expression levels of ferroptosis marker protein GPX4 and xCT (Figures 3C, 3D). Furthermore, sh-circ_0075829 led to a significant increase in the expression of immune escape marker protein IFN-γ while reducing PD-L1 expression (Figures 3C, 3D). The results obtained from the mouse model experiment were consistent with those observed in cell studies. Tumor tissue samples were validated by H&E staining (Figure 3D). In addition, CD8 was clearly localized on the cell membrane within subcutaneous tumor tissues, and its level in the sh-circ_0075829 group was significantly higher than that observed in the sh-NC group (Figures 3C, 3D). Overall, these results demonstrated that

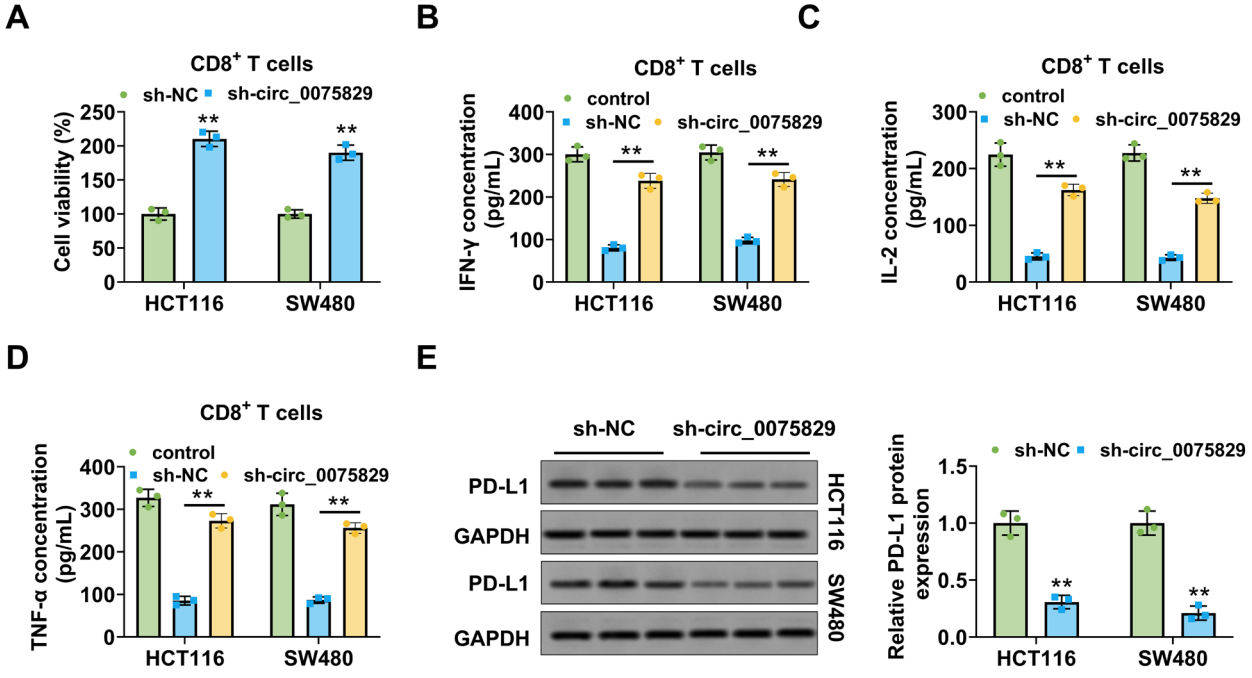

Figure 2. The effects of circ_0075829 on immune escape of colon cancer cells. HCT116 and SW480 cells were treated sh-circ_0075829 and co-cultured with CD8+ T cells 24 h. A) The cell proliferation rate of CD8+ T cell was detected by CCK-8. B) IFN-γ concentration in the supernatants of CD8+ T cell was detected by ELISA assay. C) IL-2 concentration in the supernatants of the co-culturing system was detected by ELISA assay. D) TNF-α concentration in the supernatants of the co-culturing system was detected by ELISA assay. E) Relative expression level of PD-L1 was estimated by WB. N=3. Compared with sh-NC *p<0.05, **p<0.01, ***p<0.001

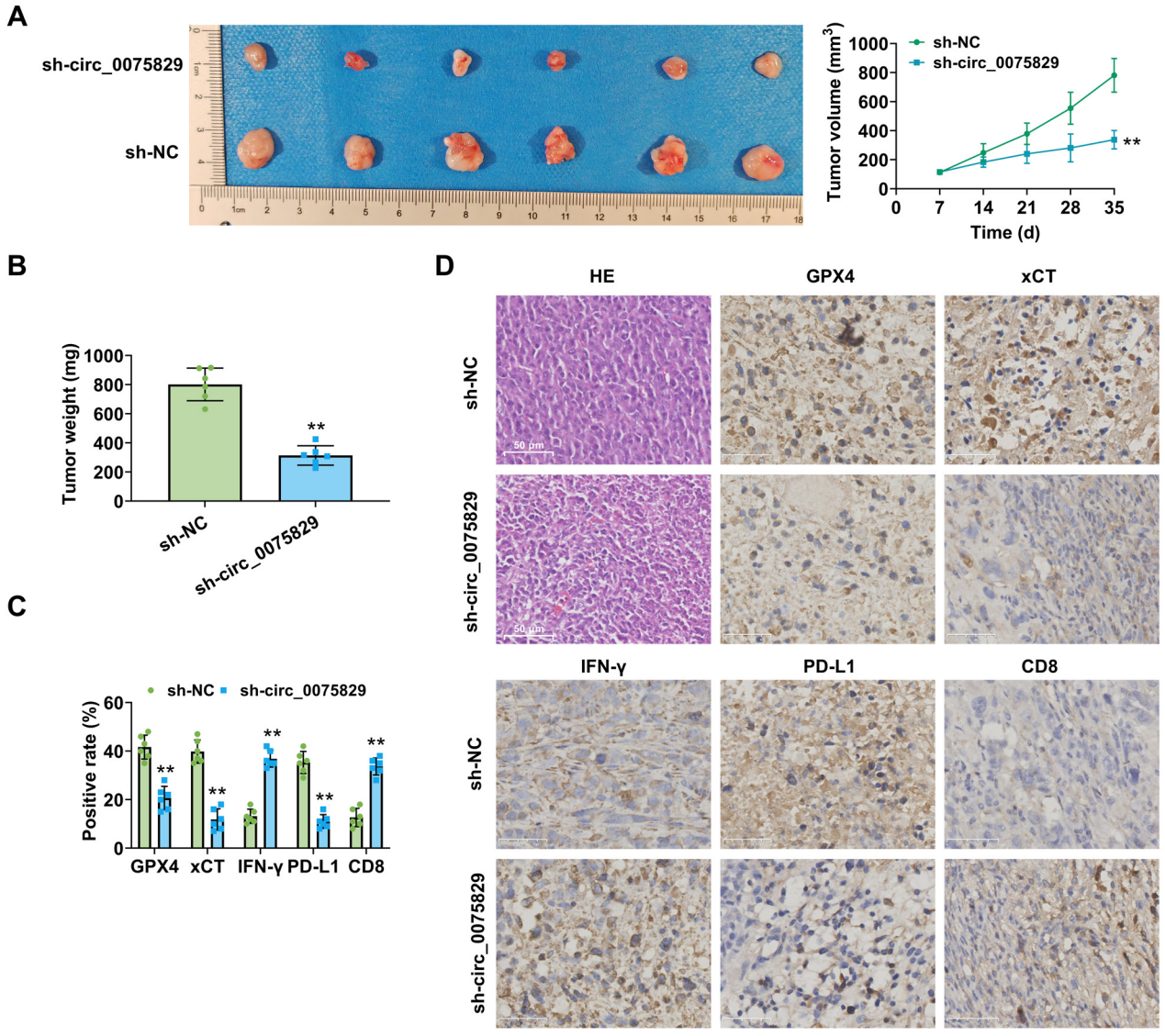

Figure 3. The effect of knockdown of circ_0075829 on ferroptosis and immune escape in colon xenograft tumor mouse models. A) Images of the tumor were recorded, and tumor volumes were measured at different times. B) Tumor weights were measured after 35 days of treatment. C, D) The expression of GPX4, xCT, IFN-γ, PD-L1, and CD8 in the mouse tumor tissues was explored by IHC staining and H&E staining of tumor tissues. N=6. Compared with sh-NC *p<0.05, **p<0.01, ***p<0.001

the knockdown of circ_0075829 effectively induced ferroptosis and inhibited immune escape *in vivo*.

circ_0075829 bound to miR-330-5p. In light of the fact that circRNA primarily functions as a miRNA sponge in the cytoplasm, we predicted that circ_0075829 and miR-330-5p had underlying binding sites by CircInteractome (https://circinteractome.nia.nih.gov) (Figure 4A). qRT-PCR analysis demonstrated that the miR-330-5p mimics significantly upregulated cellular levels of miR-330-5p compared to miR-NC (Figure 4B). And then, the luciferase activity was inhibited by miR-330-5p mimic in cells. Notably, mutating the predicted binding site between miR-330-5p and circ_0075829 abolished this inhibitory effect (Figure 4C). In the RNA pull-down assay, the biotinylated circ_0075829 probe effectively enriched miR-330-5p when compared to the NC probe (Figure 4D). Accordingly, our findings confirmed the targeting relationship between circ_0075829 and miR-330-5p.

miR-330-5p targeted TCF4. miR-330-5p and TCF4 were found to have a predicted binding site, as identified through the starBase (https://starbase.sysu.edu.cn) (Figure 5A). Subsequently, the interaction between miR-330-5p and TCF4 was validated using dual-luciferase reporter assays (Figure 5B, 5C). The WB results proved that overexpression

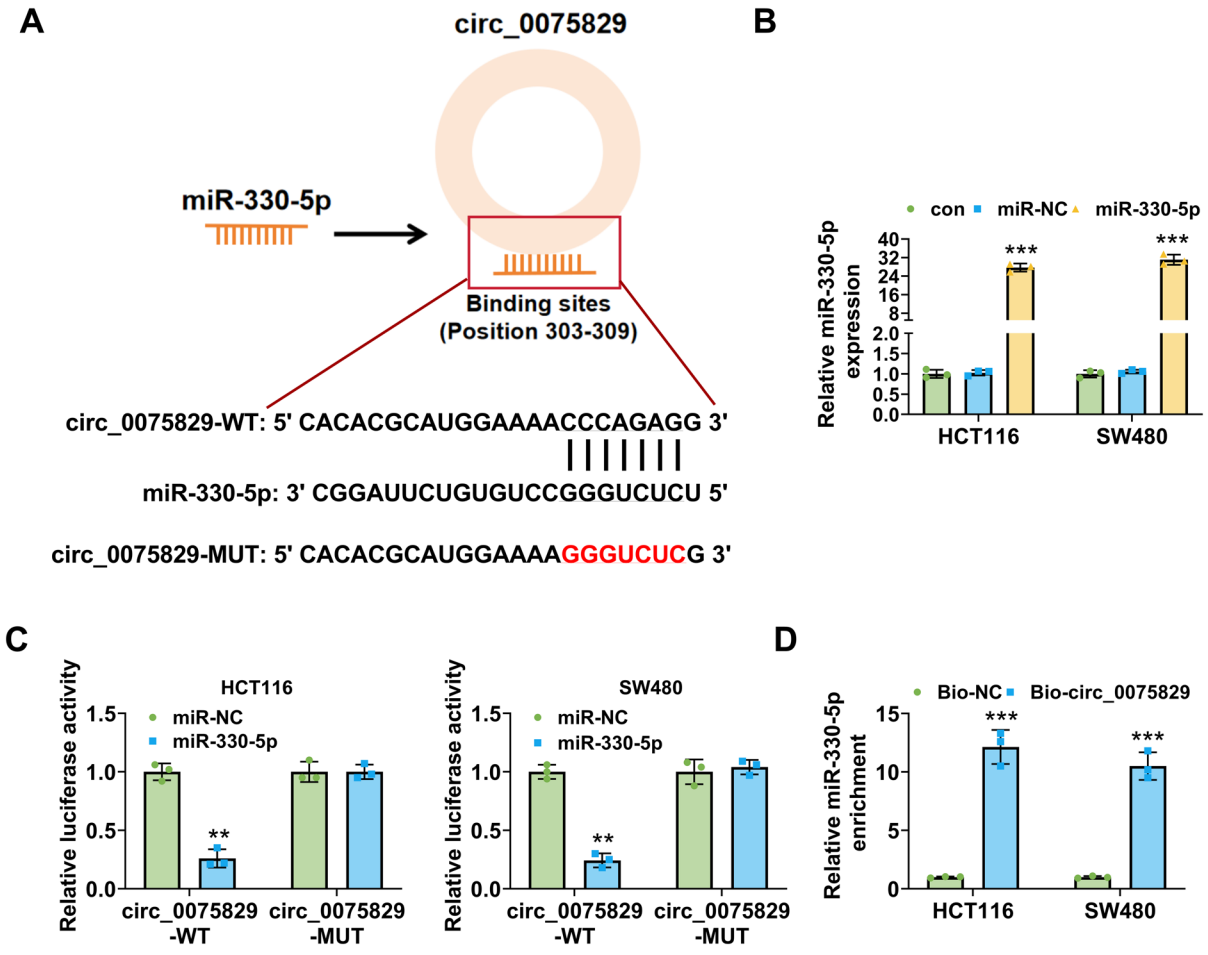

Figure 4. circ_0075829 targets miR-330-5p. A) The potential binding site of jbvb _0075829 in miR-330-5p was predicted by CircInteractome. B) qRT-PCR was used to detect the relative expression level of miR-330-5p. Compared with miR-NC *p<0.05, **p<0.01, ***p<0.001. C) The targeting relationship between circ_0075829 and miR-330-5p was verified by dual-luciferase reporter assay. Compared with miR-NC *p<0.05, **p<0.01, ***p<0.001. D) The interaction between circ_0075829 and miR-330-5p was verified by RNA pull-down assay. N=3. Compared with Bio-NC *p<0.05, **p<0.01, ***p<0.001

of miR-330-5p significantly reduced the TCF4 protein levels (Figure 5D). Additionally, qRT-PCR analysis confirmed that anti-miR-330-5p effectively downregulated miR-330-5p expression in cells (Figure 5E). Eventually, WB results indicated that sh-circ_0075829 markedly decreased the expression level of TCF4 protein. However, the expression of TCF4 protein was partially increased after co-transfection with anti-miR-330-5p (Figure 5F). Our results suggested TCF4 was a downstream target gene of miR-330-5p.

circ_0075829 regulated ferroptosis and immune escape via inducing miR-330-5p/TCF4 axis in colon cancer cells. According to the findings presented above, we hypothesized that circ_0075829 may regulate ferroptosis and immune escape in colon cancer cells through the miR-330-5p/TCF4 axis. Firstly, we constructed a TCF4 overexpression plasmid, and transfection of this plasmid effectively increased TCF4 in HCT116 and SW480 cells (Figure 6A). In terms of ferroptosis, our results indicated that knockdown of circ_0075829 significantly elevated both Fe^{2+} level and ROS level, while co-transfection with anti-miR-330-5p or TCF4 overexpression plasmid resulted in decreased Fe^{2+} level and ROS level (Figures 6B–6D). Regarding immune escape, the proliferation rate of CD8+ T cells was enhanced following co-cultured with knockdown of circ_0075829 colon cell. However, after co-transfection with anti-miR-330-5p or TCF4 overexpression plasmid, the proliferation rate of CD8+ T cells decreased again (Figure 6E). Furthermore, following the knockdown of circ_0075829, a higher level of IFN-γ was observed in co-cultured CD8+ T cells. In contrast, a lower level of IFN-γ was detected after co-transfection with anti-miR-330-5p or TCF4 overexpression plasmid (Figure 6F). Overall, our study suggested that circ_0075829 regulated ferroptosis and immune escape in colon cancer by modulating the miR-330-5p/TCF4 axis (Figure 7).

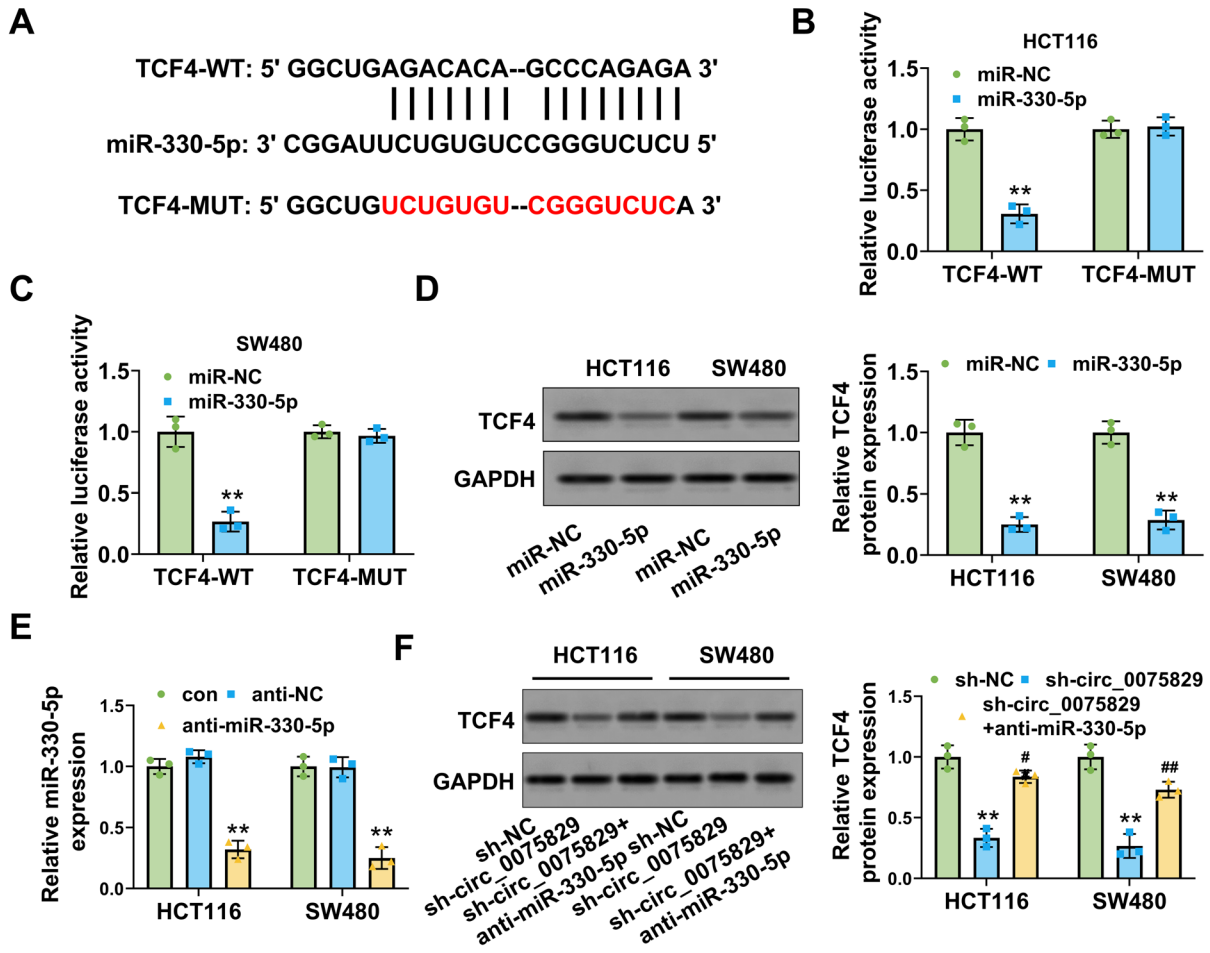

Figure 5. miR-330-5p binds to TCF4. A) Potential binding sites of miR-330-5p and TCF4 were predicted by starBase. B, C) The targeting relationship between miR-330-5p and TCF4 was verified in HCT116 and SW480 cells by dual-luciferase reporter assay. Compared with miR-NC *p<0.05, **p<0.01, ***p<0.001. D) Relative expression level of TCF4 was estimated by WB. Compared with miR-NC *p<0.05, **p<0.01, ***p<0.001. E) qRT-PCR was applied to detect the relative expression level of miR-330-5p. Compared with anti-NC *p<0.05, **p<0.01, ***p<0.001. F) The relative expression level of TCF4 was estimated by WB. N=3. Compared with sh-NC *p<0.05, **p<0.01, ***p<0.001. Compared with sh- circ_0075829 #p<0.05, ##p<0.01, ###p<0.001

Discussion

With the rapid advancement of sequencing technology, analysis technology, and databases, an increasing number of circRNAs have been recognized as integral components in the emergence and progression of various cancers [30]. Research has shown that interference with hsa_circ_0044556 can significantly reduce cell proliferation, migration, and invasion in CRC, demonstrating a positive correlation with the tumor stage [31]. Additionally, other studies have identified circRNA_100859 as an oncogene through the miR-217/HIF-1α axis in colon cancer [32]. The effects of circ_0003204 on the proliferation, motility, and angiogenesis of colon cancer cells were discussed in our previous research. This prior work also addressed the impact of circ_0003204 on tumor growth and its expression level within tumor tissue following interference. Therefore, this article will not elaborate on these findings individually. In this research, we demonstrated that circ_0075829 played a crucial role in ferroptosis and immune escape in colon cancer both in cells and in mice model.

Ferroptosis is a form of programmed cell death that is dependent on iron and is particularly prevalent in tumor cells. Research has demonstrated that ferroptosis can serve as an effective strategy for tumor treatment [33]. Various tumor suppressor genes and oncogenic signals can influence their effects through the regulation of ferroptosis. Ever-increasing studies have shown that the process of ferroptosis can be regulated by different circRNAs [34]. For instance, circLMO1 has been shown to inhibit the growth and metastasis of cervical cancer by regulating ferroptosis mediated by miR-4291/ACSL4 [35]. Li et al. [36] indicated that circSTIL obstructed ferroptosis via miR-431/SLC7A11 signaling in CRC cells. Additionally, Qin et al. [37] found that circSnx12

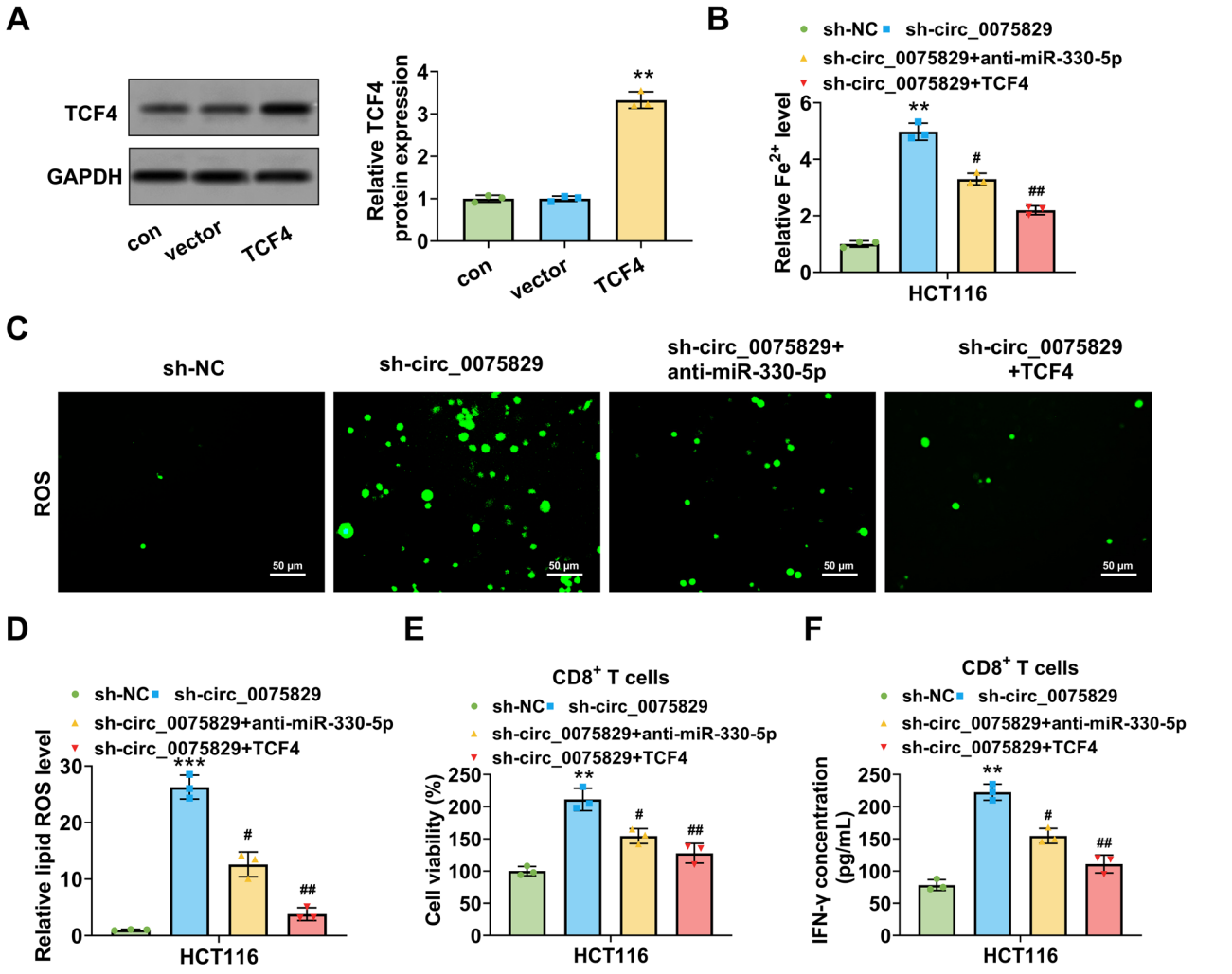

Figure 6. circ_0075829 affects ferroptosis and immune escape of colon cancer cells by the miR-330-5p/TCF4 axis. A) The relative expression level of TCF4 was estimated by WB. Compared with vector *p<0.05, **p<0.01, ***p<0.001. B) Relative level of Fe^{2+} in cells. Compared with sh-NC *p<0.05, **p<0.01, ***p<0.001. Compared with sh-circ_0075829 #p<0.05, ##p<0.01, ###p<0.001. C, D) Relative level of lipid ROS in cells. Compared with sh-NC *p<0.05, **p<0.01, ***p<0.001. Compared with sh-circ_0075829 #p<0.05, ##p<0.01, ###p<0.001. E) Cell proliferation rate was detected by CCK-8 assay. N=3. Compared with sh-NC *p<0.05, **p<0.01, ***p<0.001. Compared with sh-circ_0075829 #p<0.05, ##p<0.01, ###p<0.001. F) IFN-γ concentration was detected by ELISA assay. Compared with sh-NC *p<0.05, **p<0.01, ***p<0.001. Compared with sh-circ_0075829 #p<0.05, ##p<0.01, ###p<0.001

served on a molecular sponge for miR-194-5p, which targeted SLC7A11, thereby inhibiting ferroptosis to alleviate cisplatin resistance in ovarian cancer. In our study, the knockdown of circ_0075829 resulted in increased levels of Fe^{2+}, ROS, and MDA within cells while simultaneously decreasing SOD levels. Furthermore, silencing circ_0075829 led to reduced levels of GPX4 and xCT protein both in cells and tumor tissues.

Immune escape is a critical mechanism underlying the growth and dissemination of tumor cells. A comprehensive understanding of the mechanisms associated with tumor immune escape is essential for the development of novel immunotherapeutic strategies [38]. However, tumors have various mechanisms of immune escape, which contribute to their resilience against therapeutic interventions [39]. Existing studies have established an inevitable relationship between immune escape and the presence of diverse circRNAs. For instance, Luo et al. [40] found that hsa_circ_0000190 could enhance soluble PD-L1 expression, thereby promoting tumorigenesis and facilitating immune escape in NSCLC. Zheng et al. [41] reported that circWWC3 could indirectly elevate PD-L1 expression by increasing both the expression and secretion of IL-4, further contributing to the immune escape of breast cancer. Another study revealed that silencing circPGPEP1 inhibited the immune escape of CRC whether *in vivo* or *in vitro* [42]. Our study found that knockdown of circ_0075829 resulted in increased proliferation level of CD8+T cells co-cultured with colon cancer cells,

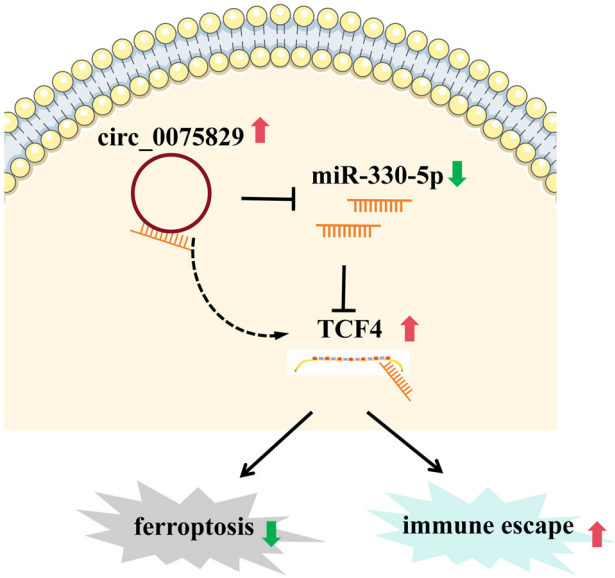

Figure 7. Schematic illustration of the molecular mechanism of circ_0075829 underlying ferroptosis and immune escape in colon cancer cells. circ_0075829 regulated the miR-330-5p/TCF4 axis by sponging miR-330-5p. Increased expression of circ_0075829 downregulated miR-330-5p expression, which upregulated TCF4 expression, thereby inhibiting ferroptosis and promoting immune escape in colon cancer cells.

along with elevated protein levels of IFN-γ and IL-2, TNF-α, while simultaneously decreasing PD-L1 protein levels. The expressions of IFN-γ and PD-L1 within tumor tissue were consistent with those observed at the cellular level.

Research has demonstrated that circRNA can function as a sponge for miRNA molecules. They act as competitive endogenous RNAs (ceRNAs), influencing the negative regulation of miRNA on target mRNA. Specifically, the overexpression of circRNA can activate miRNA target proteins [43]. The regulatory interactions between circRNAs and miRNAs in cancer have emerged as a focal point in recent studies, offering new avenues for cancer diagnosis and treatment [44]. Liu et al. [45] emphasized that hsa_circ_001783 could bind to miR-200c-3p, thereby impacting breast cancer proliferation and metastasis. Zhang et al. [46] indicated that circSATB2 could specifically regulate FSCN1 expression by directly binding to miR-326 in lung cancer cells, contributing to the progression of NSCLC. Our analysis indicated that circ_0075829 is bound to miR-330-5p through bioinformatics analysis. Subsequent luciferase reporter gene assay and RNA pull-down experiment confirmed the targeting relationship between circ_0075829 and miR-330-5p.

More interestingly, we predicted the presence of miR-330-5p binding sites in the 3' non-coding region of TCF4 using starBase and confirmed this targeting relationship through a luciferase reporter gene experiment. TCF4 plays an indispensable role in the Wnt signaling pathway and regulates the transcription processes of target genes [47]. TCF4 has been identified as having oncogenic properties in various cancers, including ovarian [48], prostate [49], and lung cancers [50]. Furthermore, it can serve as the target gene for miRNA, participating in multiple processes related to cancer occurrence and progression. Li et al. [51] indicated that lncRNA ANRIL/miR-7-5p/TCF4 axis was involved in regulating the development of T-cell acute lymphoblastic leukemia (T-ALL). Another study found that miR-190b inhibited cell proliferation and metastasis in pancreatic cancer by directly binding to MEF2C and TCF4 [52]. Additionally, TCF4 has also been reported to be upregulated in colon cancer. For instance, research indicated that overexpression of TCF4 could promote the proliferation of CRC cell lines and their resistance to doxorubicin [53]. On the other hand, a few studies have reported a certain correlation between TCF4 and ferroptosis as well as an immune escape in colon cancer [25, 54]. In this study, we also found that the knockdown of circ_0075829 led to a decrease in the expression level of TCF4 protein, which was improved following co-transfection with anti-miR-330-5p. Additionally, either anti-miR-330-5p or TCF4 overexpression vector reversed the results associated with ferroptosis and immune escape resulting from circ_0075829 knockdown. In addition, through circAltas 3.0, it could be found that miR-625 exhibited a targeted relationship with both circ_0075829 and TCF4. Therefore, further research will be conducted to elucidate the regulatory roles of miR-625, circ_0075829, and TCF4 in colon cancer. In summary, these results support our hypothesis that circ_0075829 regulates ferroptosis and immune escape processes in colon cancer via the miR-330-5/TCF4 axis.

In conclusion, this research indicated for the first time that circ_0075829 was involved in ferroptosis and immune escape through the miR-330-5p/TCF4 axis in colon cancer. Therefore, the circ_0075829/ miR-330-5p/TCF4 axis may serve as a potential target for the diagnosis and immunotherapy of colon cancer.

Supplementary information is available in the online version of the paper.

References

[1] WANG R, LIAN J, WANG X, PANG X, XU B et al. Survival rate of colorectal cancer in China: A systematic review and meta-analysis. Front Oncol 2023; 13: 1033154. https://doi.org/10.3389/fonc.2023.1033154

[2] GIOVANNUCCI E. Modifiable risk factors for colon cancer. Gastroenterol Clin North Am 2002; 31: 925–943. https://doi.org/10.1016/S0889-8553(02)00057-2

[3] ZLOBEC I, LUGLI A. Prognostic and predictive factors in colorectal cancer. J Clin Pathol 2008; 61: 561–569. https://doi.org/10.1136/jcp.2007.054858

[4] WANG Y, WEI Z, PAN K, LI J, CHEN Q. The function and mechanism of ferroptosis in cancer. Apoptosis 2020; 25: 786–798. https://doi.org/10.1007/s10495-020-01638-w

[5] NIE J, SHAN D, LI S, ZHANG S, ZI X et al. A Novel Ferroptosis Related Gene Signature for Prognosis Prediction in Patients With Colon Cancer. Front Oncol 2021; 11: 654076. https://doi.org/10.3389/fonc.2021.654076

[6] LI X, ZHANG Y. Screening ferroptosis related genes influencing prognosis of colon cancer through bioinformatics analysis. Acta Anatomica Sinica 2023; 54: 445–452. https://doi.org/10.16098/j.issn.0529-1356.2023.04.010

[7] DU X, WEN B, LIU L, WEI Y, ZHAO K. Role of immune escape in different digestive tumours. World J Clin Cases 2021; 9: 10438. https://doi.org/10.12998/wjcc.v9.i34.10438

[8] CHEN L, SHAN G. CircRNA in cancer: fundamental mechanism and clinical potential. Cancer Lett 2021; 505: 49–57. https://doi.org/10.1016/j.canlet.2021.02.004

[9] ZHANG J, LIU H, ZHAO P, ZHOU H, MAO T. Has_circ_0055625 from circRNA profile increases colon cancer cell growth by sponging miR-106b-5p. J Cell Biochem 2019; 120: 3027–3037. https://doi.org/10.1002/jcb.27355

[10] TIAN J, XI X, WANG J, YU J, HUANG Q et al. CircRNA hsa_circ_0004585 as a potential biomarker for colorectal cancer. Cancer Manag Res 2019; 11: 5413–5423. https://doi.org/10.2147/CMAR.S199436

[11] JU H, ZHAO Q, WANG F, LAN P, WANG Z et al. A circRNA signature predicts postoperative recurrence in stage II/III colon cancer. EMBO Mol Med 2019; 11: e10168. https://doi.org/10.15252/emmm.201810168

[12] WANG B, XU W, CAI Y, GUO C, ZHOU G et al. CASC15: A tumor-associated long non-coding RNA. Curr Pharm Des 2021; 27: 127–134. https://doi.org/10.2174/1381612826666200922153701

[13] WANG B, XU W, CAI Y, GUO C, ZHOU G et al. CASC15: A tumor-associated long non-coding RNA. Current Pharmaceutical Design 2021, 27: 127–134. https://doi.org/10.2174/1381612826666200922153701

[14] ZHANG Q, WANG JY, ZHOU SY, YANG SJ, ZHONG SL. Circular RNA expression in pancreatic ductal adenocarcinoma. Oncol Lett 2019; 18: 2923–2930. https://doi.org/10.3892/ol.2019.10624

[15] ZHANG X, XUE C, CUI X, ZHOU Z, FU Y et al. Circ_0075829 facilitates the progression of pancreatic carcinoma by sponging miR-1287-5p and activating LAMTOR3 signalling. J Cell Mol Med 2020; 24: 14596–14607. https://doi.org/10.1111/jcmm.16089

[16] REN D, LIU QY, LU J, WANG SC, LI YH et al. Circ0075829 is expressed in neuroblastoma tissues and inhibits cell proliferation and migration. J China Pediatr Blood Cancer 2021; 26: 261–269. https://doi.org/10.3969/j.issn.1673-5323.2021.05.002

[17] ERSON AE, PETTY EM. MicroRNAs in development and disease. Clin Genet 2008; 74: 296–306. https://doi.org/10.1111/J.1399-0004.2008.01076.X

[18] CHEN S, SHEN X. Long noncoding RNAs: functions and mechanisms in colon cancer. Mol Cancer 2020; 19: 167. https://doi.org/10.1186/s12943-020-01287-2

[19] PANDA AC. Circular RNAs act as miRNA sponges. Adv Exp Med Biol 2018; 1087: 67–79. https://doi.org/10.1007/978-981-13-1426-1_6

[20] CHEN P, YAO Y, YANG N, GONG L, KONG Y et al. Circular RNA circCTNNA1 promotes colorectal cancer progression by sponging miR-149-5p and regulating FOXM1 expression. Cell Death Dis 2020; 11: 557. https://doi.org/10.1038/s41419-020-02757-7

[21] HUANG Y, CHEN Z, ZHOU X, HUANG H. Circ_0000467 exerts an oncogenic role in colorectal cancer via miR-330-5p-dependent regulation of TYRO3. Biochem Genet 2022; 60: 1488–1510. https://doi.org/10.1007/s10528-021-10171-7

[22] WEBER MJ. New human and mouse microRNA genes found by homology search. FEBS J 2005; 272: 59–73. https://doi.org/10.1111/j.1432-1033.2004.04389.x

[23] ZHAO G, DAI GJ. Hsa_circRNA_000166 Promotes Cell Proliferation, Migration and Invasion by Regulating miR-330-5p/ELK1 in Colon Cancer. Onco Targets Ther 2020; 13: 5529–5539. https://doi.org/10.2147/OTT.S243795

[24] LU C, FU L, QIAN X, DOU L, CANG S. Knockdown of circular RNA circ-FARSA restricts colorectal cancer cell growth through regulation of miR-330-5p/LASP1 axis. Arch Biochem Biophys 2020; 689: 108434. https://doi.org/10.1016/j.abb.2020.108434

[25] CHEN Z, WANG W, HU S, SUN H, CHEN C et al. YTHDF2-mediated circYAP1 drives immune escape and cancer progression through activating YAP1/TCF4-PD-L1 axis. iScience 2023; 27: 108779. https://doi.org/10.1016/j.isci.2023.108779

[26] DONG Q, YU T, CHEN B, LIU M, SUN X et al. Mutant RB1 enhances therapeutic efficacy of PARPis in lung adenocarcinoma by triggering the cGAS/STING pathway. JCI Insight 2023; 8: e165268. https://doi.org/10.1172/jci.insight.165268

[27] MIAO Z, LI J, WANG Y, SHI M, GU X et al. Hsa_circ_0136666 stimulates gastric cancer progression and tumor immune escape by regulating the miR-375/PRKDC Axis and PD-L1 phosphorylation. Mol Cancer 2023; 22: 205. https://doi.org/10.1186/s12943-023-01883-y

[28] DIXON SJ, LEMBERG KM, LAMPRECHT MR, SKOUTA R, ZAITSEV EM et al. Ferroptosis: an iron-dependent form of nonapoptotic cell death. Cell 2012; 149: 1060–1072. https://doi.org/10.1016/j.cell.2012.03.042

[29] XIE Y, HOU W, SONG X, YU Y, HUANG J et al: Ferroptosis: process and function. Cell Death Differ 2016; 23: 369–379. https://doi.org/10.1038/cdd.2015.158

[30] GENG Y, JIANG J, WU C. Function and clinical significance of circRNAs in solid tumors. J Hematol Oncol 2018; 11: 1–20. https://doi.org/10.1186/s13045-018-0643-z

[31] JING L, WU J, TANG X, MA M, LONG F et al. Identification of circular RNA hsa_circ_0044556 and its effect on the progression of colorectal cancer. Cancer Cell Int 2020; 20: 1–13. https://doi.org/10.1186/s12935-020-01523-1

[32] ZHOU P, XIE W, HUANG H, HUANG R, TIAN C et al. circRNA_100859 functions as an oncogene in colon cancer by sponging the miR-217-HIF-1α pathway. Aging (Albany NY) 2020; 12: 13338–13353. https://doi.org/10.18632/aging.103438

[33] CHEN X, KANG R, KROEMER G, TANG D. Broadening horizons: the role of ferroptosis in cancer. Nat Rev Clin Oncol 2021; 18: 280–296. https://doi.org/10.1038/s41571-020-00462-0

[34] ARABPOUR J, REZAEI K, KHOJINI JY, RAZI S, HAYATI MJ et al. The potential role and mechanism of circRNAs in Ferroptosis: A comprehensive review. Pathol Res Pract 2024; 155203. https://doi.org/10.1016/j.prp.2024.155203

[35] OU R, LU S, WANG L, WANG Y, LV M et al. Circular RNA circLMO1 suppresses cervical cancer growth and metastasis by triggering miR-4291/ACSL4-mediated ferroptosis. Front Oncol 2022; 12: 858598. https://doi.org/10.3389/fonc.2022.858598

[36] LI Q, LI K, GUO Q, YANG T. CircRNA circSTIL inhibits ferroptosis in colorectal cancer via miR-431/SLC7A11 axis. Environ Toxicol 2023; 38: 981–989. https://doi.org/10.1002/tox.23670

[37] QIN K, ZHANG F, WANG H, WANG N, QIU H et al. circRNA circSnx12 confers Cisplatin chemoresistance to ovarian cancer by inhibiting ferroptosis through a miR-194-5p/SLC7A11 axis. BMB Rep 2023; 56: 184–189. https://doi.org/10.5483/BMBRep.2022-0175

[38] CAO J, YAN Q. Cancer epigenetics, tumor immunity, and immunotherapy. Trends Cancer 2020; 6: 580–592. https://doi.org/10.1016/j.trecan.2020.02.003

[39] BHATIA A, KUMAR Y. Cellular and molecular mechanisms in cancer immune escape: a comprehensive review. Expert Rev Clin Immunol 2014; 10: 41–62. https://doi.org/10.1586/1744666X.2014.865519

[40] LUO Y, YANG Y, CHIEN C, YARMISHYN A, ADEKUNLE ISHOLA A et al. Circular RNA hsa_circ_0000190 facilitates the tumorigenesis and immune evasion by upregulating the expression of soluble PD-L1 in non-small-cell lung cancer. Int J Mol Sci 2021; 23: 64. https://doi.org/10.3390/ijms23010064

[41] ZHENG Y, REN S, ZHANG Y, LIU S, MENG L et al. Circular RNA circWWC3 augments breast cancer progression through promoting M2 macrophage polarization and tumor immune escape via regulating the expression and secretion of IL-4. Cancer Cell Int 2022; 22: 264. https://doi.org/10.1186/s12935-022-02686-9

[42] ZHANG C, ZHANG C, LIU X, SUN W, LIU H. Circular RNA PGPEP1 induces colorectal cancer malignancy and immune escape. Cell Cycle 2023; 22: 1743–1758. https://doi.org/10.1080/15384101.2023.2225923

[43] KULCHESKI FR, CHRISTOFF AP, MARGIS R. Circular RNAs are miRNA sponges and can be used as a new class of biomarker. J Biotechnol 2016; 238: 42–51. https://doi.org/10.1016/j.jbiotec.2016.09.011

[44] VERDUCI L, STRANO S, YARDEN Y, BLANDINO G. The circ RNA–micro RNA code: emerging implications for cancer diagnosis and treatment. Mol Oncol 2019; 13: 669–680. https://doi.org/10.1002/1878-0261.12468

[45] LIU Z, ZHOU Y, LIANG G, LING Y, TAN W et al. Circular RNA hsa_circ_001783 regulates breast cancer progression via sponging miR-200c-3p. Cell Death Dis 2019; 10: 55. https://doi.org/10.1038/s41419-018-1287-1

[46] ZHANG N, NAN A, CHEN L, LI X, JIA Y et al. Circular RNA circSATB2 promotes progression of non-small cell lung cancer cells. Mol Cancer 2020; 19: 1–16. https://doi.org/10.1186/s12943-020-01221-6

[47] HRCKULAK D, JANECKOVA L, LANIKOVA L, KRIZ V, HORAZNA M et al. Wnt effector TCF4 is dispensable for Wnt signaling in human cancer cells. Genes 2018; 9: 439. https://doi.org/10.3390/genes9090439

[48] LIU L, ZENG Z, YI J, ZUO L, LV J et al. Expression and clinical significance of transcription factor 4 (TCF4) in epithelial ovarian cancer. Cancer Biomark 2019; 24: 213–221. https://doi.org/10.3233/CBM-181849

[49] LEE GT, ROSENFELD JA, KIM WT, KWON YS, PALAPATTU G et al. TCF4 induces enzalutamide resistance via neuroendocrine differentiation in prostate cancer. PloS One 2019; 14: e0213488. https://doi.org/10.1371/journal.pone.0213488

[50] SUN Y, XU J. TCF-4 regulated lncRNA-XIST promotes M2 polarization of macrophages and is associated with lung cancer. Onco Targets Ther 2019; 8055–8062. https://doi.org/10.2147/OTT.S210952

[51] LI G, GAO L, ZHAO J, LIU D, LI H et al. LncRNA ANRIL/miR-7-5p/TCF4 axis contributes to the progression of T cell acute lymphoblastic leukemia. Cancer Cell Int 2020; 20: 1–12. https://doi.org/10.1186/s12935-020-01376-8

[52] LI Y, WANG Z, ZHAO F, ZENG J, YANG X. MicroRNA 190b expression predicts a good prognosis and attenuates the malignant progression of pancreatic cancer by targeting MEF2C and TCF4. Oncol Rep 2022; 47: 1–13. https://doi.org/10.3892/or.2021.8223

[53] SUN S, YANG X, QIN X, ZHAO Y. TCF4 promotes colorectal cancer drug resistance and stemness via regulating ZEB1/ZEB2 expression. Protoplasma 2020; 257: 921–930. https://doi.org/10.1007/s00709-020-01480-6

[54] LV X, DAI Y, DAI X. IFNγ synergies with cold atmospheric plasma in triggering colorectal cancer cell ferroptosis via the IFNγ/IFNR2/APC/TCF4/GPX4 axis. Aging (Albany NY) 2023; 15: 8692–8711. https://doi.org/10.18632/aging.20498

https://doi.org/10.4149/neo_2024_240803N328

circ_0075829 regulates ferroptosis and immune escape in colon cancer cells through the miR-330-5p/TCF4 axis

Huajun FAN[1], Yu DING[2], Zhe XIAO[3], Shengbo LI[3], Yongbin ZHENG[3,*]

Supplementary Information

Supplementary Table S1. Summary of transfection oligos.

Name	Oligo Sequence
circ_0075829 shRNA 1	GATCCGCCAGCCAGGATCTGCATTTATCAA GAGTAAATGCAGATCCTGGCTGGCTTTTTT
circ_0075829 shRNA 2	GATCCGAGCCAGCCAGGATCTGCATTTCAA GAGAATGCAGATCCTGGCTGGCTCTTTTTT
circ_0075829 shRNA 3	GATCCGAGAGCCAGCCAGGATCTGCATCA AGAGTGCAGATCCTGGCTGGCTCTCTTTTTT
sh-NC	GGATCCGTTCTCCGAACGTGTCACGTTTCA AGAGAACGTGACACGTTCGGAGAATTTTTT
miR-330-5p mimic	UCUCUGGGCCUGUGUCUUAGGC
miR-NC	UUCUCCGAACGUGUCACGUTT
anti-miR-330-5p	GCCUAAGACACAGGCCCAGAGA
anti-NC	CAGUACUUUUGUGUAGUACAA

Supplementary Table S2. Primers for QRT-PCR.

Gene name	Sequence (5'–3')
hsa_circ_0075829	F: AAGAGAGCCAGCCAGGATCTG
	R: AGAAGGATGTTCAGTAGTAACCCAG
CASC15	F: CAAGAGGAATCCAGCAAAGC
	R: CATGGAGAGAGGACCTGAGC
miR-330-5p	F: GCGTCTCTGGGCCTGTGTC
	R: AGTGCAGGGTCCGAGGTATT
β-actin	F: GTCTTCCCCTCCATCGTG
	R: AGGGTGAGGATGCCTCTCTT
U6	F: CTCGCTTCGGCAGCACA
	R: AACGCTTCACGAATTTGCGT

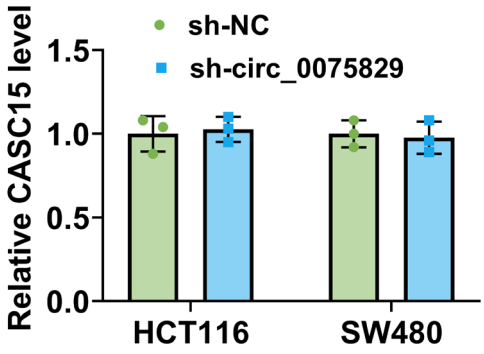

Supplementary Figure S1. The expression of CASC15 was detected by qRT-PCR.